A Novel Prognostic Model for Clear Cell Renal Cell Carcinoma with Differentially Expressed Immune-related lncRNA Pairs Based on the Cancer Genome Atlas

Chen Zhao (chen_zhao@whu.edu.cn)
Renmin Hospital of Wuhan University: Wuhan University Renmin Hospital https://orcid.org/0000-0003-1324-1375

Kewei Xiong
Central China Normal University

Fengming Liu
Central China Normal University

Xiangpan Li
Renmin Hospital of Wuhan University: Wuhan University Renmin Hospital

Research

Keywords: ccRCC, lncRNA, the Cancer Genome Atlas, prognostic model, chemosensitivity

Posted Date: August 2nd, 2021

DOI: https://doi.org/10.21203/rs.3.rs-728356/v1

Abstract

Objective: To construct a novel prognostic model of immune-related lncRNA (irlncRNA) pairs in clear cell renal cell carcinoma (ccRCC).

Methods: RNA-seq and clinical data were retrieved from The Cancer Genome Atlas (TCGA). Differentially expressed irlncRNAs (DEirlncRNAs) were obtained by co-expression strategy with immune genes. A 0-1 matrix was constructed according to DEirlncRNAs relevant expression levels. Univariate cox regression was used to select potential target pairs. Lasso regression with cross validation and multivariate cox regression were carried out to extract the final biomarker pairs for risk score calculation. Through calculating the optimal cutoff of AUCs, patients were divided into high and low risk group. Model validation was conducted by independent prognostic analysis, survival analysis, tumor-infiltrating and chemosensitivity analysis.

Results: A total of 42 DEirlncRNAs were identified and 12 target pairs were included to construct the final model. The risk score were both significantly different according to univariate ($p<0.001$, HR=1.391, 95%CI [1.313–1.475]) and multivariate cox regression ($p<0.001$, HR=1.3104, 95%CI [1.227-1.399]). The AUC reached 0.765 at 1-year, 0.724 at 3-year and 0.785 at 5-year. Patients in the high-risk group had significantly poor survival, higher level of $CD8^+$T infiltration, lower drug sensitivity of sunitinib and temsirolimus but higher sensitivity of lapatinib and pazopanib.

Conclusion: The novel prognostic model constructed by paring irlncRNAs showed an effective clinical prediction in ccRCC patients.

Introduction

Renal cell carcinoma (RCC) is one of the fatal cancers with complicated histological subtypes and roughly accounts for 80%-90% of all types of kidney tumors [1–3]. The most commonly diagnosed subtype of RCC is clear cell renal cell carcinoma (ccRCC), maintaining high mortality globally [4, 5]. Patients suffering from ccRCC are usually resistant to radiation or chemotherapy and have poor prognosis[6]. Meanwhile, molecular targeted therapy has more promising treatment in ccRCC [7]. Therefore, identification of novel effective biomarkers and molecular targets is of vital importance in tumor diagnosis and prediction.

Long non-coding RNAs (lncRNAs) are defined as RNA molecules which are more than 200 nucleotides in length and do not code for proteins. Recent studies revealed that lncRNAs have distinctive biological and pathological processes in human cancers [8–10]. A previously research has verified that lncRNAs can regulate mRNA, microRNA (miRNA) and DNA interactions, as the major class of non-coding RNAs[11]. LncRNAs involved in the immune response and showed their function as regulators in the tumor microenvironment (TME), epithelial-mesenchymal transition, microbiota, metabolism and immune cell differentiation [12, 13]. However, there is not much knowledge regarding their roles in cancer immunity

regulation. More exploration of immune-related lncRNAs (irlncRNAs) in different cancers are still required [14].

Several contributions have been made to the ccRCC diagnostic model with different biomarkers including mRNAs, miRNAs, enhancer RNAs (eRNAs), competing endogenous RNAs (ceRNAs) as well as integrated models with combinations of them[8, 15]. There were also some models with signatures related to research hotspots such as ferroptosis, N6-methyladenosine (m6A) and tumor microenvironment mainly based on the data of gene expression from online websites[16–20].

However, the inconsistency of data quality may lead to different diagnostic prediction results depending on the accurate value of expression level of identified signatures. This study aimed to develop a novel prognostic model based on differentially expressed irlncRNAs (DEirlncRNAs) between para-carcinoma and tumor cases by The Cancer Genome Atlas (TCGA) database. An independent prognostic analysis was then performed to validate the effectiveness of the constructed model. In addition, tumor immune infiltration of ccRCC and chemosensitivity were analyzed via statistical tests.

Results

Patients and clinicopathologic parameters

537 cases of ccRCC patients were obtained by TCGA as showed in Table 1. 346 of them were male and 191 were female, with the average age of 61 years (range 26–90 years)

Table 1
Patient characteristics (N = 537)

Characteristic	Sub-characteristic	Value (%)
Age (years)		61 (range = 26–90)
Gender	Male	346 (64.4)
	Female	191 (35.6)
Survival status	Dead	177 (33.0)
	Alive	360 (67.0)
Overall survival (OS)		1334 (range 0-3615) days
Grade	G1	14 (2.6)
	G2	230 (42.8)
	G3	207 (38.5)
	G4	78 (14.5)
	Gx	5 (0.9)
	unknown	3 (0.6)
Stage	Stage I	269 (50.1)
	Stage II	57 (10.6)
	Stage III	125 (23.3)
	Stage IV	83 (15.5)
	unknown	3 (0.6)
Depth of invasion (T)	T1	275 (51.2)
	T2	69 (12.8)
	T3	182 (33.9)
	T4	11 (2.0)
Distant metastasis (M)	M0	426 (79.3)
	M1	79 (14.7)
	Mx	30 (5.6)
	unknown	2 (0.4)
Lymph node metastasis (N)	N0	240 (44.7)
	N1	17 (3.2)

Characteristic	Sub-characteristic	Value (%)
	unknown	280 (52.1)

Expression processing and extraction of DEirlncRNAs

The flow chart of the study was shown as **Fig. 1**Figure 1. In terms of RNA-seq expression data from TCGA, 72 normal samples and 539 tumor samples were identified. 101 kinds of 208 irlncRNAs were selected totally (Table S1). There were 42 DEirlncRNAs (Fig. 2A) including 5 downregulated and 37 upregulated targets (Fig. 2B). The size of 0–1 matrix was 487×611, 487 was the amount of DEirlncRNA pairs and 611 referred to the whole samples (Table S2). After combination of the 537 clinical data and 539 RNA transcriptional samples, 509 cases were finally included in the further studies.

Identification of prognostic pairs and risk estimation

After intersecting the 0–1 matrix and survival data, the id of patients was set as the key and 509 samples were obtained for the univariate cox proportional hazard regression. A total of 167 DEirlncRNAs and their expression level were shown in Table S3 and Table S4. Lasso regression was perform using 167 pairs mentioned above to detect target pairs. In total, 26-DEirlncRNA pairs were identified based on the optimal value of parameter λ based on the Lasso regression (Fig. 3A). Univariate cox regression was performed again for those 26 target pairs and 12 DEirlncRNAs were determined to calculate the risk scores (Fig. 3B). The optimal cutoff to distinguish the high- and low- risk patients was 1.511 and the AUC was 0.765 with 5-year survival analysis (Fig. 3C**)**. The AUC reached 0.765 at 1 year, 0.724 at 3 years and 0.785 at 5 years respectively (Fig. 3D).

Validation of model with clinicopathologic characteristics

ccRCC patients were divided into 155 high-risk cases and 354 low-risk cases by the optimal cutoff. Kaplan-Meier analysis showed that survival of high-risk ccRCC patients was significantly shorter compared to the low-risk groups (Fig. 4A, $p < 0.001$).

The accuracy and sensitivity of the prediction model as well as other clinicopathologic characteristics was estimated by ROC. The AUC reached 0.813 of stage, 0.765 of risk score, 0.638 of age, 0.504 of gender, 0.715 of tumor grade, 0.731 of T stage and 0.734 of M stage (Fig. 4B).

Subsequently, we investigated the prognostic value of clinicopathologic characteristics and risk score. Here, age was stratified into two groups: patients ≤ 65 years and those > 65 years. The univariate cox regression demonstrated that age ($p < 0.001$, HR = 1.029, 95% CI[1.016–1.043]), tumor grade ($p < 0.001$, HR = 2.229, 95%CI[1.810–2.745]), stage($p < 0.001$, HR = 1.874[1.810–2.745]), T stage ($p < 0.001$, HR = 1.889, 95%CI[1.597–2.236]), M stage ($p < 0.001$, HR = 4.375, 95%CI[3.187–6.005]) and risk score ($p < 0.001$, HR = 1.391, 95% CI[1.313–1.475]) had prognostic value of ccRCC patients. Meanwhile, gender showed no significant difference in predicting the survival. ($p = 0.766$, HR = 0.953, 95%CI[0.692–1.311]) (Fig. 4C).

A multivariate cox regression indicated that age ($p < 0.001$, HR = 1.030, 95% CI[1.016–1.044]), tumor grade ($p = 0.042$, HR = 1.284, 95%CI[1.009–1.635]) and risk score ($p < 0.001$, HR = 1.309, 95% CI [1.225–1.398]) are independent predictor for prognosis (Fig. 4D).

The distributions of each cases' risk score and their survival status were shown in Fig. 4E and Fig. 4F.

Investigation to clinicopathologic features and gene expression with risk score

The heatmap showed correlations between clinicopathologic characteristics and risk score, which indicated that tumor grade, tumor stage, T stage and M stage were significantly related to risk score (Fig. 5A). The consequent scatter diagrams obtained by the Wilcoxon signed-rank test (Fig. 5B-G) demonstrated that tumor grade, tumor stage, T stage and M stage were significantly associated with risk score.

Moreover, all the 9 hub genes of ccRCC patients identified in a previous study (CD2, CD3D, CD8A, CXCL13, CXCR3, FASLG, GZMA, IFNG, PMCH) showed statistical differences between high- and low- risk group (Fig. 6A-I).

Analysis of ccRCC and infiltrating immune cells

Tumor infiltrating immune cells such as natural killer (NK) cell, follicular helper T cells, macrophage M1, regulatory cells (Tregs) and $CD8^+$ T cells while they had more negative associations with naive B cells, $CD4^+$ T cells and hematopoietic stem cells were included in the analysis of risk groups and tested by Spearman correlation and Wilcoxon rank-sum test using XCell, TIMER, quanTIseq, MCP-counter, EPIC, CIBERSORT and CIBERSORT-ABS algorithms.

As shown by Spearman correlation scatter plot (Fig. 7A), ccRCC patients in the high-risk group had significantly positive relation to immune cells such as follicular helper T cells, macrophage M1 and NK T cells, whereas were significantly negative related to neutrophil and hematopoietic cell.

The detailed results of correlation coefficients and p-values of immune infiltrating immune cells between high and low risk groups were showed in Table S5. The $CD4^+$ level was significantly down-regulated in the high-risk group by EPIC ($p = 9.1e-08$) and $CD8^+$ level was significantly down-regulated in the high-risk group by CIBERSORT($p = 0.00032$), CIBERSORT-ABS($p = 0.00051$), QUANTISEQ ($p = 6e-05$) and XCELL($p = 0.00045$) (Fig. 7B-F). The results of other immune cells were shown in **Figure S1**.

Significance of the Model in the antitumor drugs prediction

To evaluate the significance of the risk model in ccRCC treatment, the IC50 of common antitumor drugs was calculated. Patients in the high-risk group had lower IC50 for ccRCC-related target therapeutics such as **s**unitinib ($p = 6.3e-09$) and temsirolimus ($p = 5.4e-06$) while had higher IC50 for lapatinib ($p = 3.3e-11$) and pazopanib ($p = 0.02$) as Fig. 8 showed. It indicated that the constructed prognostic model provided possible capability for chemosensitivity prediction.

Discussion

Multiple prognostic models with molecular biomarkers and risk score calculation have been developed to predict survival time and probability of ccRCC patients [21]. However, many of them focused on the qualified expression value to stratify the risk level in ccRCC patients, which counts a lot on the accuracy of genetic testing consistence in different platforms and techniques. In this study, an improved prognostic model integrated with DElncRNA pairs rather than the specific lncRNA expression level.

To improve the previous statistical methods, we constructed a 0–1 matrix and patients were classified into high- and low- risk groups by evaluating the optimal cutoff with each AUC other than the median value. The categorical (0–1) features avoided conducting statistical tests to check the linear relations between survival outcomes and lncRNAs expression levels for cox proportional hazard regression. Model validation and reevaluation were performed through survival difference analysis, independent prognostic analysis, tumor immune infiltrating analyses and immune checkpoint inhibitors (ICIs) to manifest the effectiveness of this model. It was shown that our risk score was an independent prognostic factor had significant differences in pathological characteristics to help clinicians made an originally rough evaluation on the risk of ccRCC patients.

Among the 12 prognostic DEirlncRNA pairs, LINC00342 and LINC01094 have been researched in previous study. Some studies demonstrated that the serum level of LINC00342 was significantly elevated in patients suffered chronic kidney disease (CKD) and expression level of LINC00342 can reflect the severity of CKD [22]. Studies *in vitro* also illustrated that high expression LINC00342 could promote colorectal tumor growth and target miR-19a-3p/NPEPL1 axis and miR-545-5p/MDM2 axis, respectively [23, 24]. Furthermore, LINC00342 also contributed to the tumorigenesis in hepatocellular carcinoma patients and acted as a poor prognosis biomarker in non-small cell lung cancer[25–27].

LINC01094 can promote the development of ccRCC by upregulating SLC2A3 via miR-184 or via miR-224-5p/CHSY1 and triggers radio-resistance in ccRCC via miR-577/CHEK2/FOXM1 axis [28–30]. Acting as a ceRNA as well, LINC01094 promotes progression of ovarian cancer and glioma[31–34].

Our findings is consistent with previous studies.The constructed model demonstrated that the level of $CD4^+$ T in patients with high risk measured by EPIC was lower than those in the low risk group. On the contrary, the $CD8^+$ T cells was all higher in patients with high risk measured by CIBERORT, CIBERORT-ABS, QUANTISEQ and XCELL than those in the low risk group. The responses of $CD4^+$ and $CD8^+$ T cells are included in the immune cycle with tumor issues and they both have significant influences on the clinical prognosis [35]. Inflammatory process plays a role in RCC etiology and immunosuppressive cytokines including interleukin-10 (IL-10) have the potential to induce activation and proliferation of tumor-infiltrating CD8 + T cells and inhibits inflammatory CD4 + T cells [36].

Tyrosine kinase inhibitors (TKIs) is a family of target drugs that repress oncogenic tyrosine kinase proteins such as receptors of PDGF, EGF, FGF and VEGF, RAF proteins, cKIT, KDR, RET, FLT4, ALK and the others [37]. Sunitinib which targets at VEGFR and PDGFR has been approved for the advanced ccRCC

treatment [38]. Previous randomized trials have shown that VEGFR inhibitor pazopanib can be also used for clinical therapies [39]. A Phase research verified that the mTOR inhibitor, temsirolimus, is another option of first-line therapy [40]. In addition, EGFR and HER2 inhibitor lapatinib has been taken into ccRCC treatment in recent years [41]. This risk model illustrated that high risk patients were more significantly included in the advanced stage and grade, and they had lower IC50 level of sunitinib and temsirolimus.

However, this study has some limitations. The raw dataset was simply downloaded from TGCA database and did not contain sufficient data sample including the expression of lncRNAs, pathological characteristics and survival information for patients with ccRCC. For instance, the N stage data was unknown in 280 patients and the data related to Axitinib was missing. Meanwhile, only 79 of 537 cases were identified as M1 patients and it has influence on the analysis of chemosensitivity prediction since the TKIs are approved for advanced ccRCC treatment. Limited to sample size, it was hard to confirm the effectiveness of extracted prognostic DEirlncRNAs. To develop a more advanced and improved model with DEirlncRNA pairs, additional studies will be needed using machine learning methods to select target gene pairs within high-dimension structured data.

Conclusion

This study firstly used 0–1 matrix method to constructed a novel prognostic model with DEirlncRNA pairs for ccRCC patients via TCGA database. Different analyses were performed to evaluate the effectiveness of the model and indicated that our risk model has the potential in predicting the survival and chemosensitivity in ccRCC patients. However, further studies are still required to explore the specific molecular mechanisms of DEirlncRNAs for ccRCC initiation and progression.

Methods

Retrieval of data and target lncRNAs extraction

The RNA-seq expression (including mRNA & lncRNA) file in fragments per kilobase of exon model per million mapped fragments (FPKM) form and clinical data of 537 ccRCC patients were downloaded from TCGA (https://tcga-data.nci.nih.gov/tcga/). Two types of RNA were split according to the annotation file from Ensembl (http://asia.ensembl.org). A total of 2483 immune-related genes were retrieved from the ImmPort database (http://www.immport.org) which provides shared data for immunological analysis. The irlncRNAs were identified via co-expression with immune-related genes (ir-genes) of which the Pearson correlation coefficients more than 0.8 and p-value less than 0.001 were set as the thresholds. DEirlncRNAs were identified with a false discovery rate (FDR) less than 0.05 and the absolute value of log Fold Change (|logFC|) more than 1.5 through limma package of R. Strawberry Perl was used to create structured data downloaded from websites. R (version of 3.6.3), a free programming language for statistics, was used to conduct the model construction, data analyses and plots.

Construction of DEirlncRNA pairs

A 0-1 matrix was applied to build DEirlncRNA pairs cyclically as follow:

$$i \mid j \triangleq f(i,j) = \begin{cases} 1, & \text{mean expression of } i \text{ more than } j \\ 0, & \text{otherwise} \end{cases}$$

which means the expression level of the *i*th DEirlncRNA was more than the *j*th one (*i*<*j*). The form "*i* | *j*" was considers as the DEirlncRNA pair. The detailed form could be formulated as:

$$\begin{bmatrix} x_{11} & x_{12} & \cdots & x_{1n} \\ x_{21} & x_{22} & \cdots & x_{2n} \\ \vdots & \vdots & \ddots & \vdots \\ x_{m1} & x_{m2} & \cdots & x_{mn} \end{bmatrix}_{m \times n}$$

where x_{ij}=0 or 1; *m* represented the sample size and *n* represented the number of DEirlncRNA pairs.

The following numerator represented the amounts of expression quantity was 0 or 1 of each DEirlncRNA pair among all samples:

$$ratio\_0 = \frac{\sum expression\ level\ was\ 0}{\sum the\ amount\ of\ samples}, \qquad ratio\_1 = \frac{\sum expression\ level\ was\ 1}{\sum the\ amount\ of\ samples}$$

When the ratio of DEirlncRNA pair was more than 20% of total pairs, it was defined as a valid match.

Selection of target pairs and establishment of prognostic model

After excluding the samples with overall survival (OS) less than 30 days, the constructed DEirlncRNA-pair matrix was combined with the survival information of ccRCC patients. A univariate proportional hazard regression was performed to detect the prognostic signature pairs. The threshold was set as p-value less

than 0.01. Then a 10-fold Lasso regression was run with 5000 cycles to construct the final prognostic model.

The risk score of each patient could be calculated as

$$risk\ score = \sum \alpha_i P_i$$

where α_i was the value abstracted from the 0-1 matrix, and the P_i was the coefficients of Lasso regression. Receiver operating characteristic (ROC) curve was carried out and the area under curve (AUC) was calculated. The maximum AUC value was defined as the optimal cutoff of the risk score and patients were divided into high and low risk groups. Kaplan-Meier (KM) was analyzed to predict the OS of ccRCC patients in the high- or low-risk group through survival ROC package.

Validation of the Constructed Risk Model

To analyze the significant difference of survival situation of high- or low- risk groups, the log-rank test was performed through survival package. Samples with Mx and Gx which represented unclear clinicopathologic results were excluded from univariate and multivariate cox analysis. N staging was also omitted because of the data deficiency. The independent prognostic analysis was performed with the calculated risk score and five clinical factors: age, gender, tumor stage, T and M stage. Then AUCs were compared to validate the superiority of constructed model and the distribution of patients in different groups was visualized by showing the risk curve and scatter plot. The correlation of clinicopathologic features and interested gene expression was analyzed between the high- and low- risk groups by Wilcox two-side test.

To validate the prognostic value of this model, the hub genes of ccRCC identified in a previous study (CD2, CD3D, CD8A, CXCL13, CXCR3, FASLG, GZMA, IFNG, PMCH) were carried out using our risk score model [42].

Exploration of tumor infiltrating immune cells

Immune infiltration information of ccRCC patients based on TCGA identities which provides expression profiles of immune cells was downloaded from TIMER 2.0 (http://timer.comp-genomics.org)[43-46]. Spearman correlation coefficients were calculated to investigate the association between the risk level and immune cells containing XCell, TIMER, quanTIseq, MCP-counter, EPIC, CIBERSORT and CIBERSORT-ABS algorithms. The difference of each immune cell between high- and low- risk groups was estimated by Wilcoxon rank-sum test, of which the p-value was set as 0.001 as the threshold.

Analysis of the model in chemosensitivity

The RNA-seq expression of ccRCC tumor samples from TCGA cohort was used to analyze the chemosensitivity through pRRophetic package[47]. Recommendations for RCC treatment like lapatinib, pazopanib, sunitinib and vinblastine were included in the comparison analysis. Wilcoxon test was performed to evaluate the difference between the high- and low- risk groups according to the value of 50% maximal inhibitory concentration (IC50).

Abbreviations

RCC: renal cell carcinoma

ccRCC: clear cell renal cell carcinoma

TCGA: The Cancer Genome Atlas

lncRNA: long non-coding RNA

DEirlncRNAs: differentially expressed irlncRNAs ()

irlncRNA: immune-related lncRNA

AUC: area under the curve

TME: tumor microenvironment

miRNA: microRNA

eRNA: enhancer RNA

ceRNA: competing endogenous RNA

m6A: N6-methyladenosine

ir-genes: immune-related genes

FDR: false discovery rate

ROC: Receiver operating characteristic

OS: overall surviva

Declarations

• Ethics approval and consent to participate

Not applicable.

• Consent to publish

The authors confirm that the work described has not been published before and this publication has been approved by all co-authors.

• Availability of data and materials

Data used in this study can be downloaded from TCGA (https://tcga-data.nci.nih.gov/tcga/), Ensembl (http://asia.ensembl.org) and the ImmPort database (http://www.immport.org).

• Competing interests

The authors declare no competing interests.

• Funding

This study was supported by “the Fundamental Research Funds for the Central Universities 2042020kf0084”.

• Authors' Contributions

Chen Zhao and Xiangpan Li designed the study. Kewei Xiong and Fengming Liu collected study data and performed statistical analysis. Chen Zhao and Kewei Xiong wrote manuscript draft. All authors read and approved the manuscript.

• Acknowledgements

None.

References

1. Linehan WM, Ricketts CJ. The Cancer Genome Atlas of renal cell carcinoma: findings and clinical implications. Nat Rev Urol. 2019;16(9):539–52.
2. Escudier B, Porta C, Schmidinger M, Rioux-Leclercq N, Bex A, Khoo V, Grunwald V, Gillessen S, Horwich A. Renal cell carcinoma: ESMO Clinical Practice Guidelines for diagnosis, treatment and follow-updagger. Ann Oncol. 2019;30(5):706–20.

3. Zhu WK, Xu WH, Wang J, Huang YQ, Abudurexiti M, Qu YY, Zhu YP, Zhang HL, Ye DW. Decreased SPTLC1 expression predicts worse outcomes in ccRCC patients. J Cell Biochem. 2020;121(2):1552–62.
4. Chen L, Peng T, Luo Y, Zhou F, Wang G, Qian K, Xiao Y, Wang X. ACAT1 and Metabolism-Related Pathways Are Essential for the Progression of Clear Cell Renal Cell Carcinoma (ccRCC), as Determined by Co-expression Network Analysis. Front Oncol. 2019;9:957.
5. Qin S, Shi X, Wang C, Jin P, Ma F. Transcription Factor and miRNA Interplays Can Manifest the Survival of ccRCC Patients. Cancers (Basel) 2019, 11(11).
6. Ma J, Li M, Chai J, Wang K, Li P, Liu Y, Zhao D, Xu J, Yu K, Yan Q, et al. Expression of RSK4, CD44 and MMP-9 is upregulated and positively correlated in metastatic ccRCC. Diagn Pathol. 2020;15(1):28.
7. Song Y, Huang J, Shan L, Zhang HT. Analyses of Potential Predictive Markers and Response to Targeted Therapy in Patients with Advanced Clear-cell Renal Cell Carcinoma. Chin Med J (Engl). 2015;128(15):2026–33.
8. Hong W, Liang L, Gu Y, Qi Z, Qiu H, Yang X, Zeng W, Ma L, Xie J. Immune-Related lncRNA to Construct Novel Signature and Predict the Immune Landscape of Human Hepatocellular Carcinoma. Mol Ther Nucleic Acids. 2020;22:937–47.
9. Theis M, Paszkowski-Rogacz M, Weisswange I, Chakraborty D, Buchholz F. Targeting Human Long Noncoding Transcripts by Endoribonuclease-Prepared siRNAs. J Biomol Screen. 2015;20(8):1018–26.
10. Wang J, Su Z, Lu S, Fu W, Liu Z, Jiang X, Tai S. LncRNA HOXA-AS2 and its molecular mechanisms in human cancer. Clin Chim Acta. 2018;485:229–33.
11. Charles Richard JL, Eichhorn PJA. Platforms for Investigating LncRNA Functions. SLAS Technol. 2018;23(6):493–506.
12. Chen YG, Satpathy AT, Chang HY. Gene regulation in the immune system by long noncoding RNAs. Nat Immunol. 2017;18(9):962–72.
13. Denaro N, Merlano MC, Lo Nigro C. Long noncoding RNAs as regulators of cancer immunity. Mol Oncol. 2019;13(1):61–73.
14. Robinson EK, Covarrubias S, Carpenter S. The how and why of lncRNA function: An innate immune perspective. Biochim Biophys Acta Gene Regul Mech. 2020;1863(4):194419.
15. Jiang H, Chen H, Wan P, Song S, Chen N. Downregulation of enhancer RNA EMX2OS is associated with poor prognosis in kidney renal clear cell carcinoma. Aging. 2020;12(24):25865–77.
16. Zhou J, Wang J, Hong B, Ma K, Xie H, Li L, Zhang K, Zhou B, Cai L, Gong K. Gene signatures and prognostic values of m6A regulators in clear cell renal cell carcinoma - a retrospective study using TCGA database. Aging. 2019;11(6):1633–47.
17. Zhao Y, Tao Z, Chen X. Identification of a three-m6A related gene risk score model as a potential prognostic biomarker in clear cell renal cell carcinoma. PeerJ. 2020;8:e8827.

18. Luo Y, Shen D, Chen L, Wang G, Liu X, Qian K, Xiao Y, Wang X, Ju L. Identification of 9 key genes and small molecule drugs in clear cell renal cell carcinoma. Aging. 2019;11(16):6029–52.
19. Wu G, Wang Q, Xu Y, Li Q, Cheng L. A new survival model based on ferroptosis-related genes for prognostic prediction in clear cell renal cell carcinoma. Aging. 2020;12(14):14933–48.
20. Xu WH, Xu Y, Wang J, Wan FN, Wang HK, Cao DL, Shi GH, Qu YY, Zhang HL, Ye DW. Prognostic value and immune infiltration of novel signatures in clear cell renal cell carcinoma microenvironment. Aging. 2019;11(17):6999–7020.
21. Qu L, Wang ZL, Chen Q, Li YM, He HW, Hsieh JJ, Xue S, Wu ZJ, Liu B, Tang H, et al. Prognostic Value of a Long Non-coding RNA Signature in Localized Clear Cell Renal Cell Carcinoma. Eur Urol. 2018;74(6):756–63.
22. Liu C, Xu Y, Wu X, Zou Q. Clinical Significance Of Linc00342 Expression In The Peripheral Blood Lymphocytes Of Patients With Chronic Kidney Disease. Int J Nephrol Renovasc Dis. 2019;12:251–6.
23. Shen P, Qu L, Wang J, Ding Q, Zhou C, Xie R, Wang H, Ji G. LncRNA LINC00342 contributes to the growth and metastasis of colorectal cancer via targeting miR-19a-3p/NPEPL1 axis. Cancer Cell Int. 2021;21(1):105.
24. Miao Z, Liu S, Xiao X, Li D. LINC00342 regulates cell proliferation, apoptosis, migration and invasion in colon adenocarcinoma via miR-545-5p/MDM2 axis. Gene. 2020;743:144604.
25. Bai Z, Li H, Li C, Sheng C, Zhao X. Integrated analysis identifies a long non-coding RNAs-messenger RNAs signature for prediction of prognosis in hepatitis B virus-hepatocellular carcinoma patients. Medicine. 2020;99(40):e21503.
26. Chen QF, Kong JL, Zou SC, Gao H, Wang F, Qin SM, Wang W. LncRNA LINC00342 regulated cell growth and metastasis in non-small cell lung cancer via targeting miR-203a-3p. Eur Rev Med Pharmacol Sci. 2019;23(17):7408–18.
27. Tang H, Zhao L, Li M, Li T, Hao Y. Investigation of LINC00342 as a poor prognostic biomarker for human patients with non-small cell lung cancer. J Cell Biochem. 2019;120(4):5055–61.
28. Xu H, Wang X, Wu J, Ji H, Chen Z, Guo H, Hou J. Long Non-coding RNA LINC01094 Promotes the Development of Clear Cell Renal Cell Carcinoma by Upregulating SLC2A3 via MicroRNA-184. Front Genet. 2020;11:562967.
29. Jiang Y, Zhang H, Li W, Yan Y, Yao X, Gu W. FOXM1-Activated LINC01094 Promotes Clear Cell Renal Cell Carcinoma Development via MicroRNA 224-5p/CHSY1. Mol Cell Biol 2020, 40(3).
30. Jiang Y, Li W, Yan Y, Yao X, Gu W, Zhang H. LINC01094 triggers radio-resistance in clear cell renal cell carcinoma via miR-577/CHEK2/FOXM1 axis. Cancer Cell Int. 2020;20:274.
31. Xu J, Zhang P, Sun H, Liu Y. LINC01094/miR-577 axis regulates the progression of ovarian cancer. J Ovarian Res. 2020;13(1):122.
32. Li XX, Yu Q. Linc01094 Accelerates the Growth and Metastatic-Related Traits of Glioblastoma by Sponging miR-126-5p. Onco Targets Ther. 2020;13:9917–28.

33. Zhu B, Liu W, Liu H, Xu Q, Xu W. LINC01094 Down-Regulates miR-330-3p and Enhances the Expression of MSI1 to Promote the Progression of Glioma. Cancer Manag Res. 2020;12:6511–21.
34. Dong X, Fu X, Yu M, Li Z. Long Intergenic Non-Protein Coding RNA 1094 Promotes Initiation and Progression of Glioblastoma by Promoting microRNA-577-Regulated Stabilization of Brain-Derived Neurotrophic Factor. Cancer Manag Res. 2020;12:5619–31.
35. Ostroumov D, Fekete-Drimusz N, Saborowski M, Kuhnel F, Woller N. CD4 and CD8 T lymphocyte interplay in controlling tumor growth. Cell Mol Life Sci. 2018;75(4):689–713.
36. Autio K, Oft M. Pegylated Interleukin-10: Clinical Development of an Immunoregulatory Cytokine for Use in Cancer Therapeutics. Curr Oncol Rep. 2019;21(2):19.
37. Law V, Knox C, Djoumbou Y, Jewison T, Guo AC, Liu Y, Maciejewski A, Arndt D, Wilson M, Neveu V, et al. DrugBank 4.0: shedding new light on drug metabolism. Nucleic Acids Res. 2014;42(Database issue):D1091–7.
38. Huang D, Ding Y, Li Y, Luo WM, Zhang ZF, Snider J, Vandenbeldt K, Qian CN, Teh BT. Sunitinib acts primarily on tumor endothelium rather than tumor cells to inhibit the growth of renal cell carcinoma. Cancer Res. 2010;70(3):1053–62.
39. Coppin C, Kollmannsberger C, Le L, Porzsolt F, Wilt TJ. Targeted therapy for advanced renal cell cancer (RCC): a Cochrane systematic review of published randomised trials. BJU Int. 2011;108(10):1556–63.
40. Chowdhury S, Choueiri TK. Recent advances in the systemic treatment of metastatic papillary renal cancer. Expert Rev Anticancer Ther. 2009;9(3):373–9.
41. Rini BI. Lapatinib therapy for patients with advanced renal cell carcinoma. Nat Clin Pract Oncol. 2008;5(11):626–7.
42. Xu T, Ruan H, Song Z, Cao Q, Wang K, Bao L, Liu D, Tong J, Yang H, Chen K, et al. Identification of CXCL13 as a potential biomarker in clear cell renal cell carcinoma via comprehensive bioinformatics analysis. Biomed Pharmacother. 2019;118:109264.
43. Li T, Fu J, Zeng Z, Cohen D, Li J, Chen Q, Li B, Liu XS. TIMER2.0 for analysis of tumor-infiltrating immune cells. Nucleic Acids Res. 2020;48(W1):W509–14.
44. Li T, Fan J, Wang B, Traugh N, Chen Q, Liu JS, Li B, Liu XS. TIMER: A Web Server for Comprehensive Analysis of Tumor-Infiltrating Immune Cells. Cancer Res. 2017;77(21):e108–10.
45. Li B, Severson E, Pignon JC, Zhao H, Li T, Novak J, Jiang P, Shen H, Aster JC, Rodig S, et al. Comprehensive analyses of tumor immunity: implications for cancer immunotherapy. Genome Biol. 2016;17(1):174.
46. Sturm G, Finotello F, Petitprez F, Zhang JD, Baumbach J, Fridman WH, List M, Aneichyk T. Comprehensive evaluation of transcriptome-based cell-type quantification methods for immuno-oncology. Bioinformatics. 2019;35(14):i436–45.
47. Geeleher P, Cox N, Huang RS. pRRophetic: an R package for prediction of clinical chemotherapeutic response from tumor gene expression levels. PLoS One. 2014;9(9):e107468.

Figures

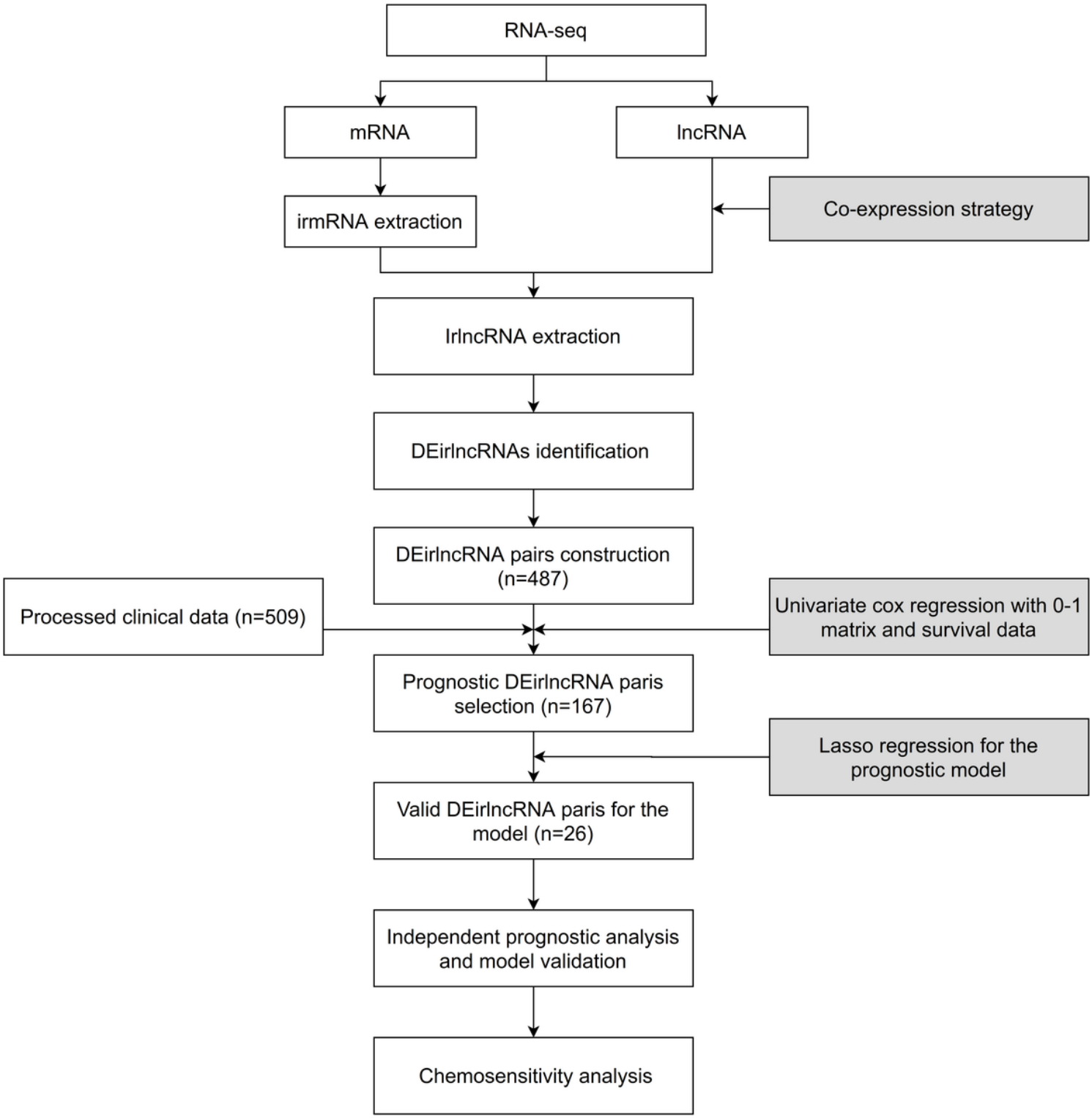

Figure 1

The flow chart of the study.

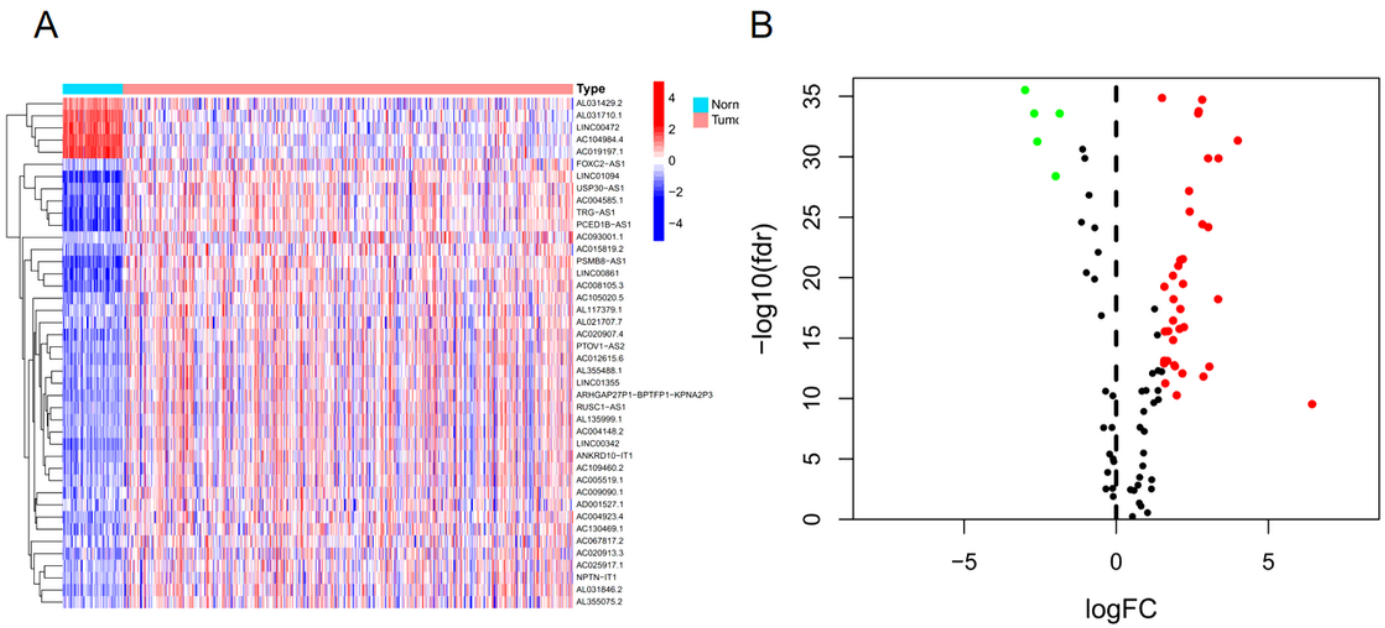

Figure 2

Screen of identified DEirlncRNAs. (A) Heatmap of all results; (B) Volcano plot of all results. (Green: downregulated, Red: upregulated).

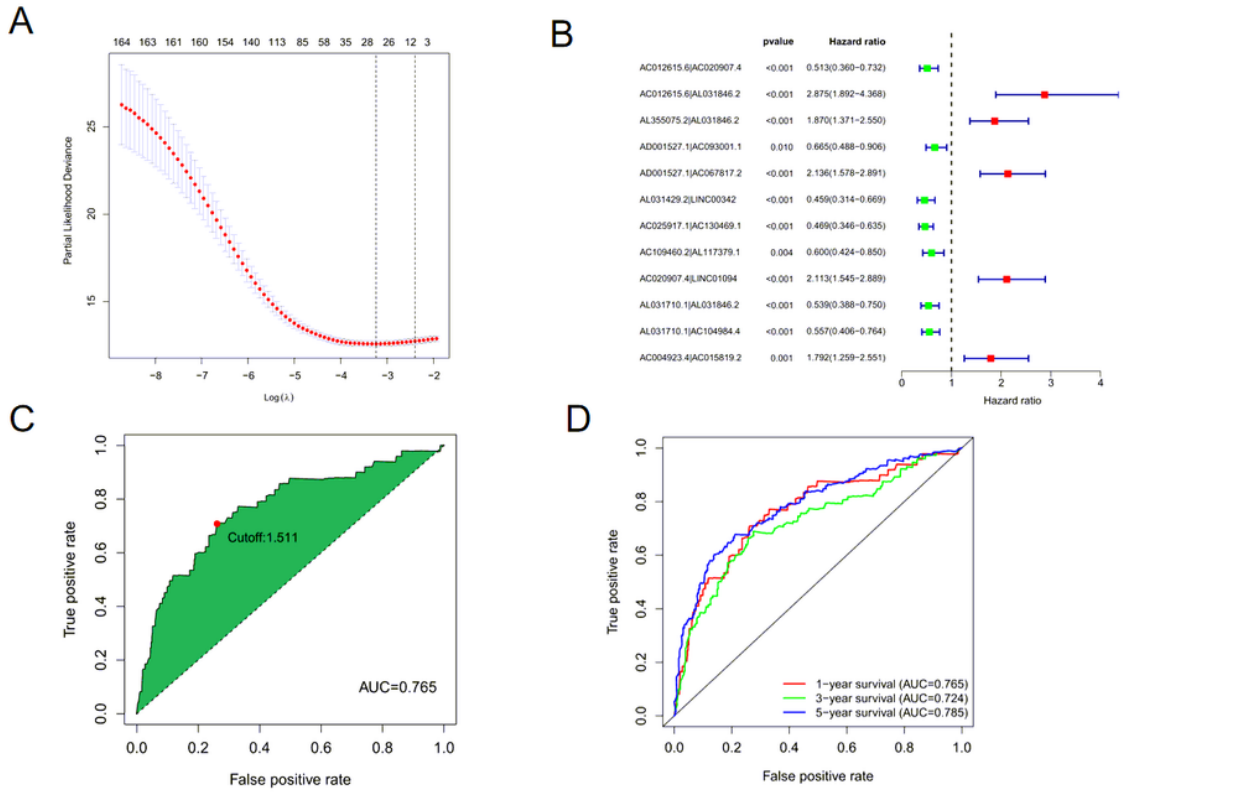

Figure 3

Results of prognostic model establishment. (A) 26-DEirlncRNA pairs were identified based on the optimal value of parameter λ; (B) A forest map showed 12 DEirlncRNA pairs determined by Cox proportional hazard regression; (C) A 5-year ROC curves with other common clinical characteristics showed the optimal cutoff value of 1.511 ; (D) The 1-, 3-, and 5-year ROC curves and AUC values of the optimal model.

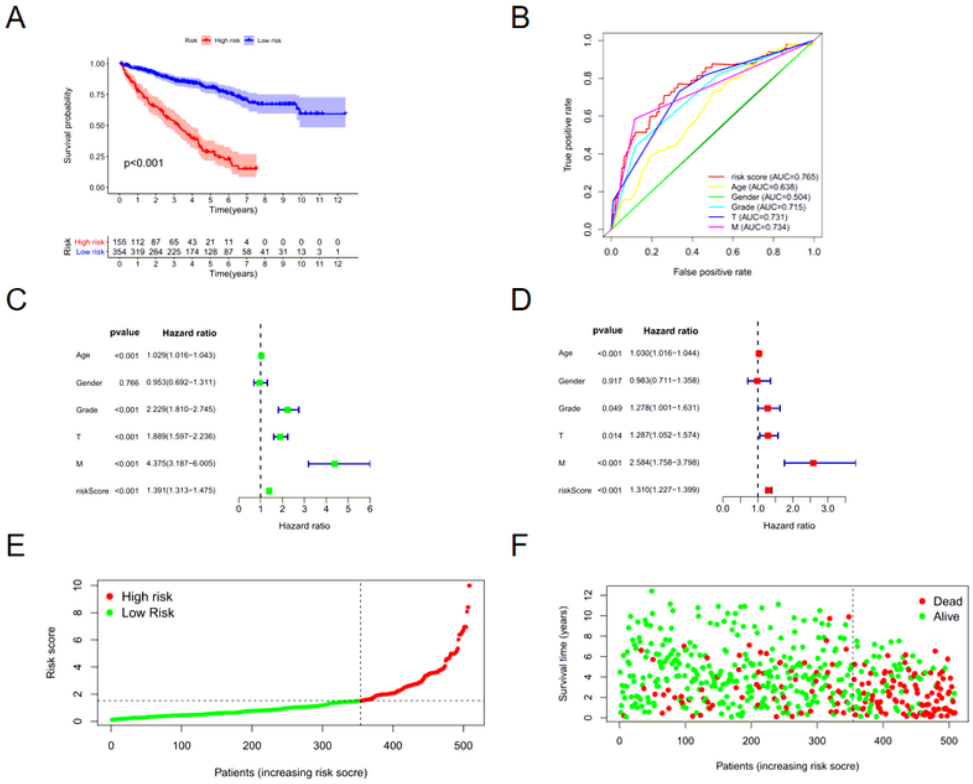

Figure 4

Validation of model with risk scores. (A) Kaplan-Meier curves showed the ccRCC patients of low risk group had a better survival compared to that of high-risk groups (p<0.001); (B) ROC curves showed the accuracy of the model with risk score and other common clinicopathological characteristics; (C) The univariate cox regression demonstrated that age, tumor grade, stage, T stage, M stage and risk score had prognostic value of ccRCC patients; (D) The multivariate cox regression indicated that age, tumor grade and risk score are independent predictor for prognosis; (E) The continuously increasing curve showed the border of risk score and the number of patients; (F) A scatter plot showed the distribution of the relation of each case' survival status and risk score.

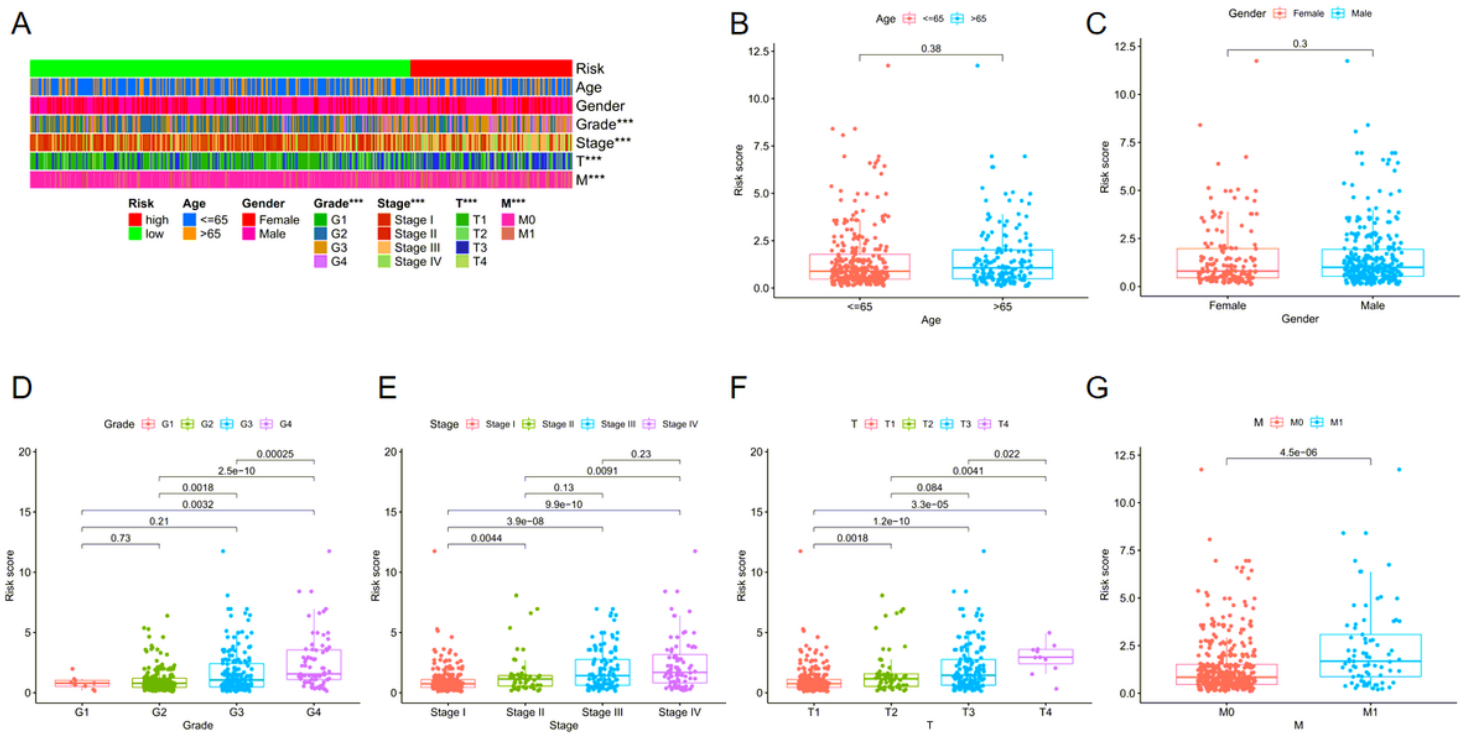

Figure 5

Correlation between clinical characteristics and risk score. (A) Heatmap of the relations (B-G) Box plot of relations between age, gender, tumor grade, tumor stage, T stage as well as M stage and risk score, respectively.

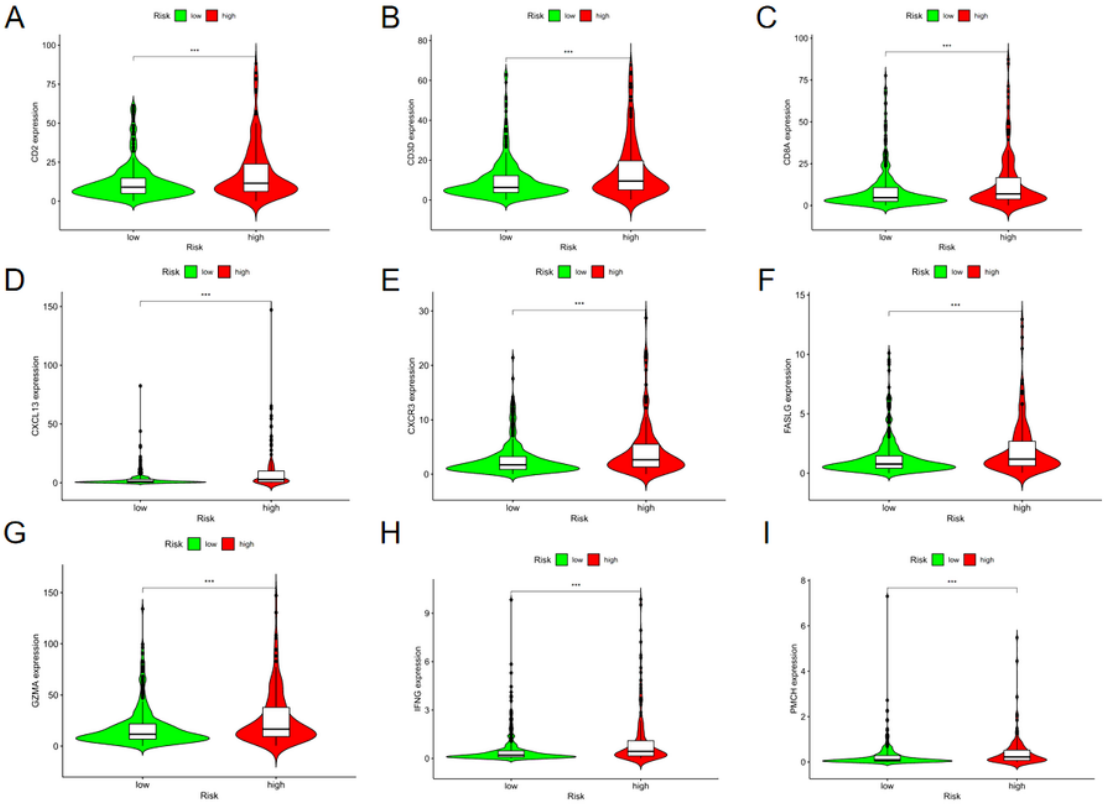

Figure 6

Hub gene (A) CD2, (B) CD3D, (C) CD8A, (D) CXCL13, (E) CXCR3, (F) FASLG, (G) GZMA, (H) IFNG, (I) PMCH expression are significantly associated with risk score, respectively.

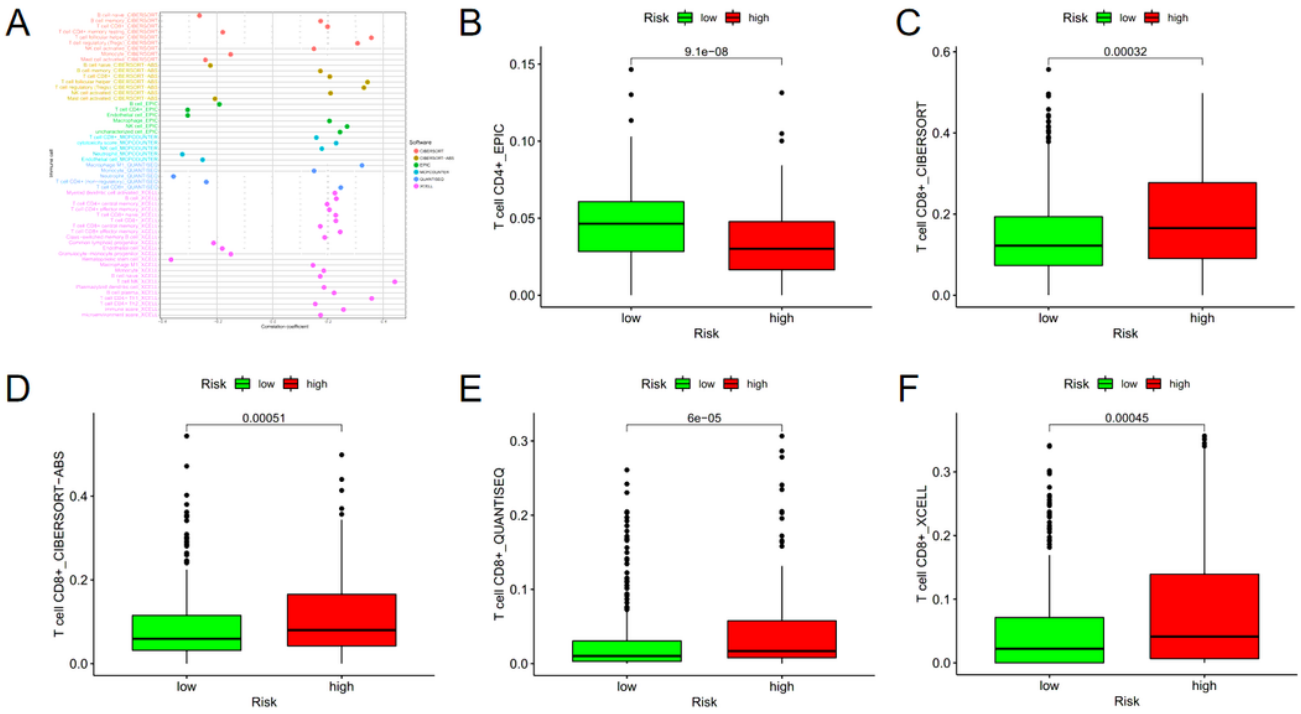

Figure 7

Results of ccRCC immune infiltrating. (A) ccRCC patients in the high-risk group had significantly positive relation to immune cells such as follicular helper T cells, macrophage M1 and NK T cells, whereas were significantly negative related to neutrophil and hematopoietic cell. (B) The level of CD4+ T cells estimated by EPIC was significantly down-regulated in the high-risk group (p=9.1e-08). (C) The level of CD8+ T cells estimated by CIBERSORT was significantly up-regulated in the high-risk group (p=0.00032). (D) The level of CD8+ T cells estimated by CIBERSORT-ABS was significantly up-regulated in the high-risk group (p=0.00051). (E) The level of CD8+ T cells estimated by QUANTISEQ was significantly up-regulated in the high-risk group (p=6e-05). (F) The level of CD8+ T cells estimated by XCELL was significantly up-regulated in the high-risk group (p=0.00045).

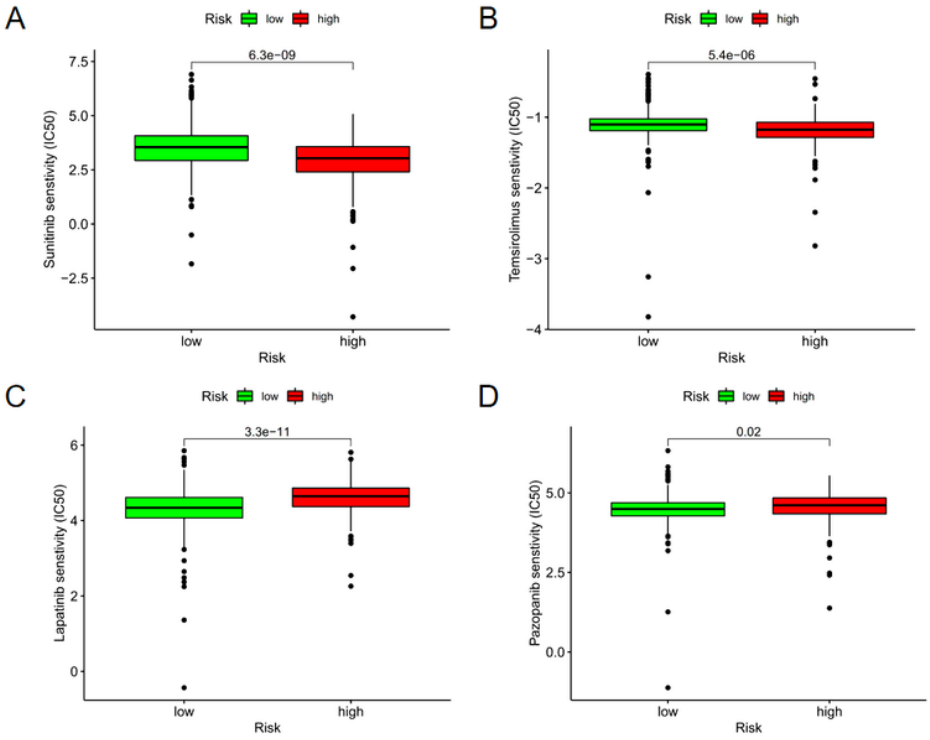

Figure 8

The model acted as a potential predictor for chemosensitivity as high-risk scores were related to lower IC50 for sunitinib (p=6.3e-09) and temsirolimus (p=5.4e-06), whereas they were associated with higher IC50 for lapatinib (p=3.3e-11) and pazopanib (p=0.02).

Supplementary Files

This is a list of supplementary files associated with this preprint. Click to download.

- TableS1.xlsx

- TableS2.xlsx
- TableS3.xlsx
- TableS4.xlsx
- TableS5.xlsx